Available online at www.sciencedirect.com

ScienceDirect

JOURNAL OF IRON AND STEEL RESEARCH, INTERNATIONAL. 2015, 22(11): 996-1001

Plate Shape Control Theory and Experiment for 20-high Mill

Zheng-wen YUAN[1,2], Hong XIAO[1,2]

(1. National Engineering Research Center for Equipment and Technology of Cold Strip Rolling, Yanshan University, Qinhuangdao 066004, Hebei, China; 2. College of Mechanical Engineering, Yanshan University, Qinhuangdao 066004, Hebei, China)

Abstract: Roll flattening theory is an important part of plate shape control theories for 20-high mill. In order to improve the accuracy of roll flattening calculation for 20-high mill, a new and more accurate roll flattening model was proposed. In this model, the roll barrel was considered as a finite length semi-infinite body. Based on the boundary integral equation method, the numerical solution of the finite length semi-infinite body under the distributed force was obtained and an accurate roll flattening model was established. Coupled with roll bending model and strip plastic deformation, a new and more accurate plate control model for 20-high mill was established. Moreover, the effects of the first intermediate roll taper angle and taper length were analyzed. The tension distribution calculated by analytical model was consistent with the experimental results.

Key words: 20-high mill; roll flattening; finite length semi-infinite body; boundary integral equation method; plate shape control

The 20-high cold rolling mill, which has rolls arranged as cluster, is widely used in thin strip rolling process. In the past years, some researches on 20-high mill have been made to improve the quality of the plate shape. The roll deformation and plate shape can be obtained by finite element analysis (FEA) and analytical model. FEA can be used to calculate roll deformation accurately[1], but it is difficult for online calculation due to its time-consuming. Compared with FEA, the analytical model can greatly shorten the calculation time and the calculation accuracy is acceptable.

Roll deformation theory is the core part of plate shape control theories, which includes roll flattening and roll bending deformation. Foppl formula[2] and semi-infinite body model[3] are the most popular analytical models in the roll flattening calculation. With Foppl formula as the roll flattening model, Yu et al.[4] established a roll deformation model of 20-high mill. Coupled with the metal plastic deformation, the effects of the first intermediate roll shifting and taper, AS-U-ROLL, tension, work roll crown and the second intermediate non-drive roll crown on strip edge drop were analyzed. Cho and Hwang[5] deduced an analytical model for predicting plate shape of 20-high Sendzimir mill. The model, which was developed on the basis of the predictions from finite element simulation, was applied to the analysis of roll deformation in a 20-high Sendzimir mill under some special conditions, such as rigid outer rolls and without roll shifting, etc. A numerical model for plate shape prediction of 20-high Sendzimir mill is established by Shin et al.[6], which is based on the contact element method, and the effects of AS-U-ROLL and first intermediate roll were considered. A numerical model based on the contact element method and Foppl formula for the prediction of plate shape for 20-high mill was obtained by Shin et al. Wang et al.[7] investigated the effect of different AS-U-ROLL control schemes on the plate shape defects in 20-high mill rolling process using the semi-infinite body model as the roll flattening model. A simulation model for predicting the shapes of cold-rolled strips in 20-high Sendzimir mills was developed by Hara et al.[8]; by this model, improvement of quarter buckles was shown difficult merely by conventional shape control actuators.

However, contact position and roll flattening are very complicated because the rolls of 20-high mill are arranged as cluster. The current roll flattening model cannot obtain accurate result for 20-high mill. Foppl formula is derived based on the assumption of ignoring the strain along the axial direction, which leads to the low-precision of Foppl formula. Semi-infinite body model is derived based on Boussinesq solution[9]. In the semi-infinite body model, the effects of shear stress and normal stress along the axial direction are considered. However, since the roll barrel has a finite length, the roll flattening calculated by semi-infinite body model has a great deviation from actual situation, especially near the barrel edges.

In the past years, some improvements have been done to increase the accuracy of the calculation, such as

Foundation Item: Item Sponsored by National Natural Science Foundation of China (51474190); Natural Sceince Foundation of Hebei Province of China (E2015203311)

Biography: Zheng-wen YUAN, Doctor; **E-mail:** yzwysu@ysu.edu.cn; **Received Date:** June 20, 2014

Corresponding Author: Hong XIAO, Doctor, Professor; **E-mail:** xhh@ysu.edu.cn

Berger[10], Zhou[11,12] and Hacquin[13]. But most modified semi-infinite body models were based on the result obtained by FEA, which is practical, and there were too many assumptions and lack theoretical support. In this paper, the deformation of a finite length semi-infinite body under the distributed force was obtained based on boundary integral equation method. The results were used in roll flattening calculation of strip rolling mill and more accurate roll flattening results were predicted. Based on the roll flattening model, a new roll deformation model of 20-high mill was deduced. Coupled with the strip plastic deformation, more plate shape value was obtained.

1 Establishment of Roll Flattening Model Based on Finite Length Semi-infinite Body

The displacement field of a finite length semi-infinite body under the distributed force $t_3(Q)$ is shown in Fig. 1. The length of the finite length semi-infinite body is L along X_1-axis and infinite along X_2-axis and X_3-axis positive direction.

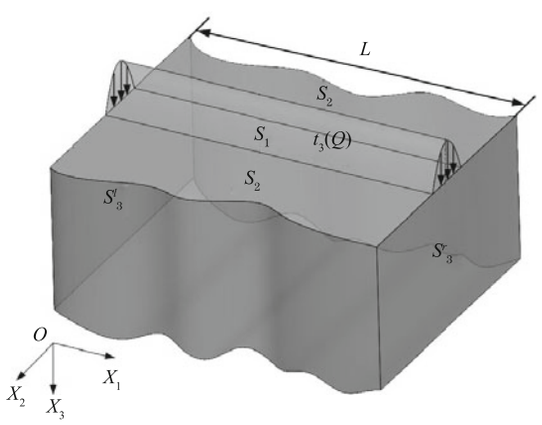

Fig. 1 Finite length semi-infinite body under the distributed force

In order to solve the problem in Fig. 1, the boundary integral equation is established as Eq. (1)[14].

$$C_{ij}(P)u_j(P)+\int_S t_{ij}^*(P,Q)u_j(Q)\mathrm{d}S=\int_S u_{ij}^*(P,Q)t_j(Q)\mathrm{d}S \tag{1}$$

where, P is load point; $C_{ij}(P)$ is a function about Kronecker symbol; $u_j(P)$ is the displacement of P in j direction; Q is field point position vectors; $u_j(Q)$ and $t_j(Q)$ are displacement vector and traction vector; S is the boundary; and $t_{ij}(P,Q)$ and $u_{ij}(P,Q)$ are fundamental solutions for the tractions and displacements in j direction of Q due to a unit load in i direction of P.

Eq. (1) can be derived by Betti reciprocal theorem, which is applicable for both surface and internal points. The fundamental solutions can be chosen from Kelvin solution or Mindlin solution in the isotropic case. In this paper, Mindlin solution[15] was used.

Considering the rolling actual situation and roll barrel contact feature, Eq. (1) can be dispersed and simplified as Eq. (2)[16].

$$\begin{aligned}u_3(P_i)=&\sum_{j=1}^{n}\int_S u_{33}^*(P_i,Q)T_j(X_2)\mathrm{d}S-\\&u_1(P_1)\int_{S^l}t_{31}^*(P_i,Q)f'(X_2,X_3)\mathrm{d}S-\\&u_1(P_n)\int_{S^r}t_{31}^*(P_i,Q)f'(X_2,X_3)\mathrm{d}S-\\&u_3(P_1)\int_{S^l}t_{33}^*(P_i,Q)f(X_2,X_3)\mathrm{d}S-\\&u_3(P_n)\int_{S^r}t_{33}^*(P_i,Q)f(X_2,X_3)\mathrm{d}S\\&(i=1,2,\cdots n)\end{aligned} \tag{2}$$

where, $f(X_2,X_3)$ and $f'(X_2,X_3)$ are the lateral surface displacement decay functions, and the detailed derivation process is shown in Ref. [16].

Based on FEA, it is concluded that the displacement decay law is related to the distance from action points of force and the contact arc length ($2b$). Considering all the factors and the simulation results of FEA, the lateral surface displacement decay functions are expressed as follows.

$$f(X_2,X_3)=0.258\cdot\left(\ln\frac{1\,000b}{b+\sqrt{X_3^2+(1.8X_2)^2}}\right)^{0.7} \tag{3}$$

$$f'(X_2,X_3)=0.055\cdot\left(\ln\frac{1\,000b}{b+\sqrt{X_3^2+(1.56X_2)^2}}\right)^{1.5} \tag{4}$$

Based on Eqs. (2)–(4), the roll flattening can be obtained. The new model is compared with semi-infinite body model, Foppl formula and FEA. The result shows that the flattening calculated by the new model is more close to FEA than the other models[16].

2 Establishment of Plate Shape Control Model

2.1 Establishment of roll deformation model

Based on the new roll flattening model, a new 20-high mill roll deformation model can be established. The roll deformation of 20-high mill includes roll bending deformation, roll flattening deformation among rolls, and roll flattening between work roll and strip. Considering the complexity of 20-high mill roll deformation, the roll barrels of 20-high mill are divided into a series of equal units. The load and deformation of each unit are analyzed separately. The 20-high mill deformation discrete model is shown in Fig. 2, in which $\boldsymbol{P}_j$ is the rolling force of unit j, and $\boldsymbol{q}_j$, $\boldsymbol{q}_j'$ and $\boldsymbol{q}_j''$ are pressure between rolls of the first, second and third layers, respectively.

The 20-high mill rolls are set as a cluster, as shown in Fig. 3. In order to analyze roll deformation, force analysis should be carried out for the special structure of rolls, and then the force equilibrium, deflection deformation, torque equilibrium, and displacement coordination function can be established. In Fig. 3, α_1–α_7 are the angles between rolls center connection and horizontal line, and e is eccentricity.

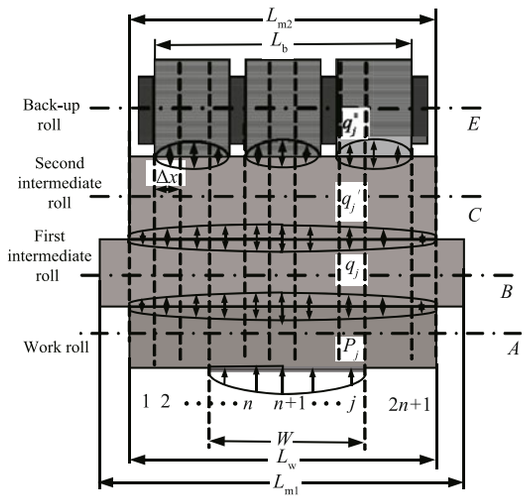

Fig. 2 Discrete model of the roll deformation for 20-high mill

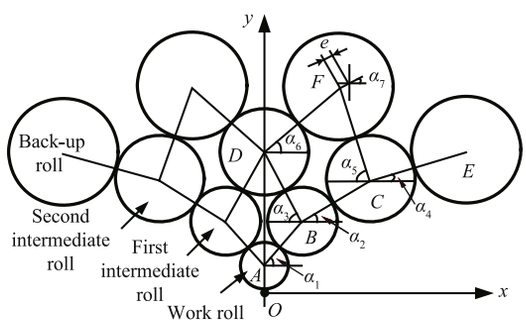

Fig. 3 20-high mill rolls arrangement

Taking roll *B* as an example, the force equilibrium, deflection deformation, torque equilibrium, and displacement coordination function are established respectively. The analysis methods of the other roll are similar, so repeat is unnecessary.

Based on the position of rolls setting, the force equilibrium relationship of roll *B* along different directions can be shown as follows[7].

A-B:

$$-q_{AB}+q_{BC}\cos(\alpha_1-\alpha_2)+q_{BD}\cos(180^\circ-\alpha_3-\alpha_1)=0 \tag{5}$$

C-B:

$$-q_{AB}\cos(\alpha_1-\alpha_2)+q_{BC}+q_{BD}\cos(180^\circ-\alpha_3-\alpha_2)=0 \tag{6}$$

D-B:

$$-q_{AB}\cos(180^\circ-\alpha_1-\alpha_3)+q_{BC}\cos(180^\circ-\alpha_3-\alpha_2)+q_{BD}=0 \tag{7}$$

where, q is pressure between rolls, and subscripts are roll number.

Not only the force equilibrium relationship, but also the equilibrium condition, the discrete units of 20-high mill rolls need to be met, which are shown as follows.

A-B:

$$\sum_{i=1}^{n}-q_{AB}x(i)+q_{BC}x(i)\cos(\alpha_1-\alpha_2)-q_{BD}(i)x(i)\cos(180^\circ-\alpha_3-\alpha_1)=0 \tag{8}$$

B-C:

$$\sum_{i=}^{n}q_{BC}(i)x(i)+q_{BD}(i)x(i)\cos(180^\circ-\alpha_3-\alpha_2)-q_{AB}(i)x(i)\cos(\alpha_1-\alpha_2)=0 \tag{9}$$

B-D:

$$\sum_{i=1}^{n}q_{BC}(i)x(i)\cos(180^\circ-\alpha_3-\alpha_2)+q_{BD}(i)x(i)-q_{AB}(i)x(i)\cos(180^\circ-\alpha_1-\alpha_3)=0 \tag{10}$$

where, $x(i)$ is the coordinate of roll. Based on the force equilibrium relationship, the deflection deformation of unit *i* on roll *B* can be obtained as follows.

A-B:

$$Y_{BA}(i)=\sum_{j=}^{n}G_{BL}(i,j)[-q_{AB}(j)+q_{BC}(j)\cos(\alpha_1-\alpha_2)+q_{BD}(j)\cos(180^\circ-\alpha_3-\alpha_1)] \tag{11}$$

C-B:

$$Y_{BC}(i)=\sum_{j=1}^{n}G_{BL}(i,j)\big[-q_{AB}(j)\cdot\cos(\alpha_1-\alpha_2)+q_{BC}(j)+q_{BD}(j)\cos(180^\circ-\alpha_3-\alpha_2)\tag{12}$$

D-B:

$$Y_{BD}(i)=\sum_{j=}^{n}G_{BL}(i,j)[-q_{AB}(j)\cos(180^\circ-\alpha_1-\alpha_3)+q_{BC}(j)\cos(180^\circ-\alpha_3-\alpha_2)+q_{BD}(j)] \tag{13}$$

where, $Y_{BA}(i)$ is the deflection of unit *i* on roll *B* along connection line between roll *B* and *A*; q_{AB} is pressure of unit *j* between roll *B* and *A*; and $G_{BL}(i,j)$ is roll *B* bending influence coefficient caused by discrete load.

Based on the setting position of the 20-high mill rolls, displacement coordination function of two adjacent rolls along connection line of rolls′ centers is established as follows.

$$Y_m(i)=Y_n(i)+[Y_{mn}(\text{mid})-Y_{mn}(i)]-\frac{\Delta D_{mn}}{2}+\beta_{mn}x(i) \tag{14}$$

where, $Y_m(i)$ and $Y_n(i)$ are deflection of unit *i* on roll *m* and *n* along connection line between them; Y_{mn}(mid) and $Y_{mn}(i)$ are roll flattening of roll center and unit *i* along connection line between roll *m* and *n*, which can be obtained by the new roll flattening model proposed in this paper; β_{mn} is the rigid corner between adjacent two rolls; and ΔD_{mn} is the roll crown between adjacent two rolls.

The loaded exit gap distribution between two work rolls is described as follows.

$$h_i=h_{\text{mid}}-Y_{\text{w}}^{\text{u}}(i)-Y_{\text{w}}^{\text{d}}(i)+\frac{\Delta D_{\text{w}i}^{\text{u}}}{2}+\frac{\Delta D_{\text{w}i}^{\text{d}}}{2}-2(Y_{\text{ws}}(\text{mid})-Y_{\text{ws}}(i)) \tag{15}$$

where, h_i is the thickness of unit i; h_{mid} is the thickness of the strip center; $Y_{\text{w}}^{\text{u}}(i)$ and $Y_{\text{w}}^{\text{d}}(i)$ are the up and down work roll deflection of unit i; ΔD_{wi}^{u} and ΔD_{wi}^{d} are the up and down work roll crown; and $Y_{\text{ws}}(\text{mid})$ and $Y_{\text{ws}}(i)$ are the roll flattening between work roll and strip of roll center and unit i[17].

2.2 Coupling of roll deformation and strip plastic deformation

In order to analyze the plate shape in rolling process, the roll elastic deformation and strip plastic deformation should be taken into account. Based on the variational method deduced by Lian[18], the strip plastic deformation and the tension distribution can be obtained. Considering the back and front tension distribution, the rolling force can be calculated. Hill formula[19] was used as the rolling force model, which considers the rolling elastic and plastic regions and is applicable for thin strip rolling process. At last, the roll deformation and strip plastic deformation are coupled together. When the cycling condition of the two models meets for convergence, the plate shape result is output. The calculation block diagram of 20-high mill plate shape calculation model is shown in Fig. 4.

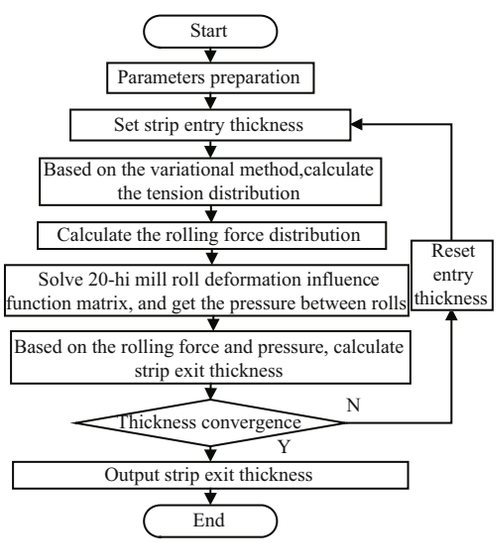

Fig. 4 20-high mill plate shape calculation model block diagram

3 Results and Discussion

Based on the plate shape calculation model for 20-high mill, the plate shape effect law of 20-high mill will be obtained. And the results will be proved by rolling test in the same condition. The calculation parameters are listed in Table 1.

3.1 Influence of taper angle of the first intermediate roll

As shown in Fig. 5, the plate shape results are obtained by the new calculation model in 0.001 3, 0.002 3, and 0.003 3 taper angle of the first intermediate roll. In this calculation, strip entry and exit thickness are 0.4 mm and 0.307 mm; strip width is 110 mm; front and back tension are 68 MPa and 80 MPa; there is a taper on the right of the first intermediate roll, and the taper length is 50 mm.

Table 1 Main design data of 20-high mill

Parameter	Value
Work roll	ϕ(8−12) mm×158 mm
First intermediate roll	ϕ22 mm×170 mm
Second intermediate roll	ϕ36 mm×158 mm
Back up roll	ϕ60 mm×40 mm×3
Strip width	50−120 mm
Strip thickness	0.4 mm
Strip yield strength	500 MPa

Based on the force distribution in the first layer, it can be found that the contact area between work roll and first intermediate roll gradually concentrated in the middle of the rolls as the taper angle increases, which causes the increase of uneven pressure. Larger pressure happened in the 1/3 of strip center and the pressure difference between roll center and edge increases accordingly. Similarly, the difference of rolling force between strip center and edge increases as well. As a result, the deflection of work roll decreases, and the lateral rigidity of 20-high mill increases; then strip center wave increases.

A test was carried out under the same condition. As shown in Fig. 6, the strip center wave trend increases as the taper angle increases from 0.001 3 to 0.003 3. It is concluded that the tension distribution calculated by analytical model is consistent with test result.

3.2 Influence of taper length of the first intermediate roll

As shown in Fig. 7, the plate shape results are obtained by the new calculation model in 30 mm, 50 mm, 60 mm, and 70 mm taper length of the first intermediate roll. In this calculation, strip entry and exit thickness are 0.4 mm and 0.307 mm; strip width is 110 mm; front and back tension are 68 MPa and 80 MPa; there is a taper on the right of the first intermediate roll, and the taper angle is 0.001 3.

When the taper length is 30 mm, the flat barrel length of the first intermediate roll is longer than strip width. As shown in Fig. 7, it can be found that the pressure between rolls distribution is relatively flat, and the pressure over the strip width range is great, which causes that the deflection of work roll is relatively large, and the lateral rigidity of 20-high mill is relatively small. The rolling force at the strip edge is strong, and the strip edge drop and edge wave are serious. When the taper length increases to 70 mm gradually, the taper section of the first intermediate roll has been overlapped 45 mm within the strip width. Based on the pressure distribution in the first layer, it can be found that the contact length between work roll and the first intermediate roll is 80 mm, and

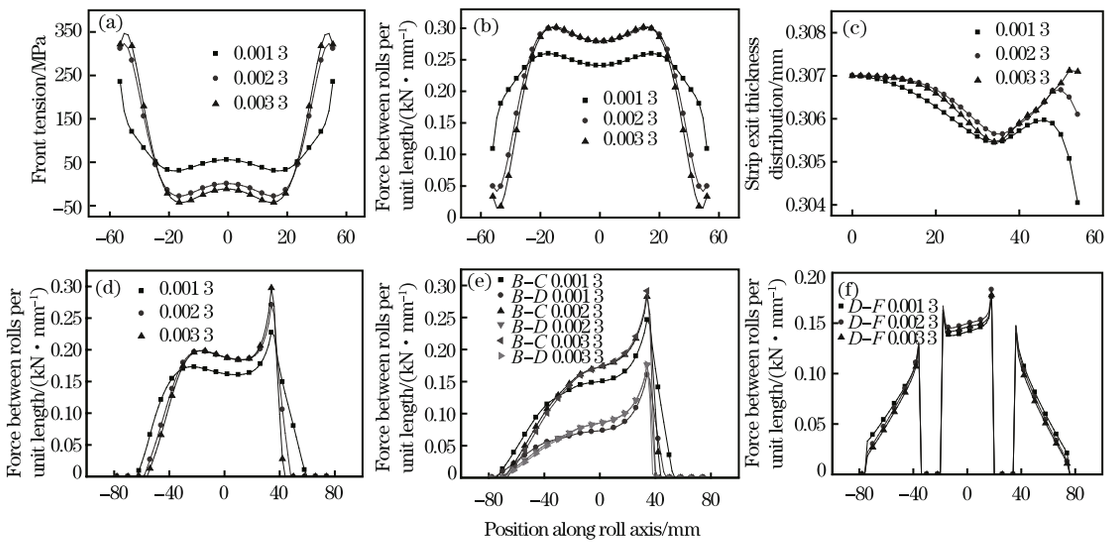

Fig. 5 Calculation results for different taper angles

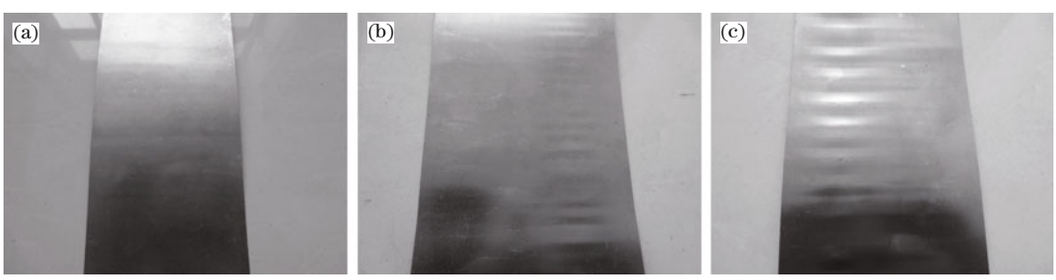

Fig. 6 Test results for different taper angles of 0.001 3 (a), 0.002 3 (b) and 0.003 3 (c)

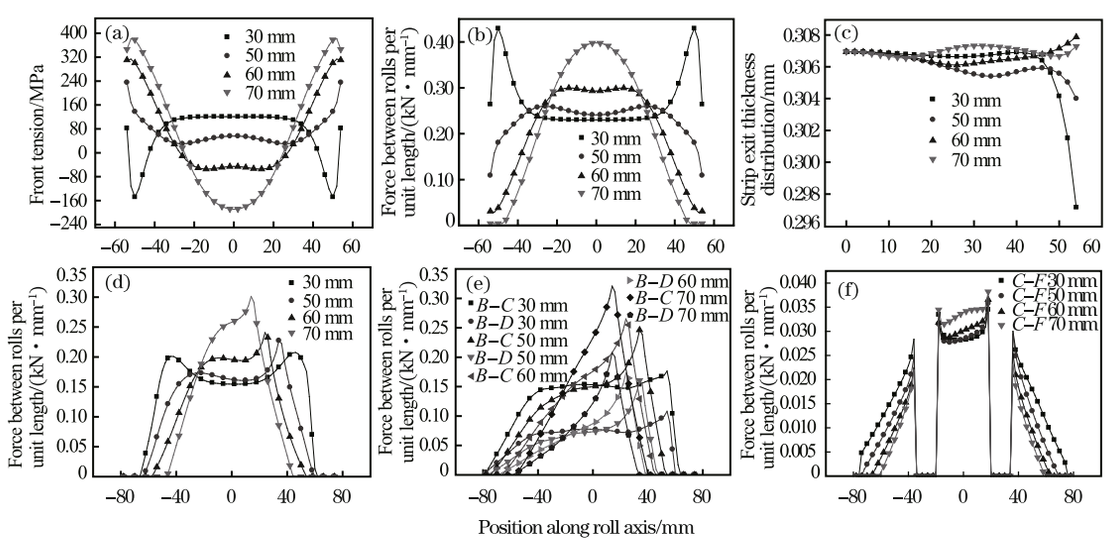

Fig. 7 Calculation results for different taper lengths

most pressure concentrates in 40 mm around the roll center. As a result, the deflection of work roll decreases, and the lateral rigidity of 20-high mill increases, so the strip center wave increases.

A test was carried out under the same condition. As shown in Fig. 8, the plate shape changes gradually from edge wave to center wave as the taper length increases from 30 mm to 70 mm. It is concluded that the tension distribution calculated by analytical model is consistent with test result.

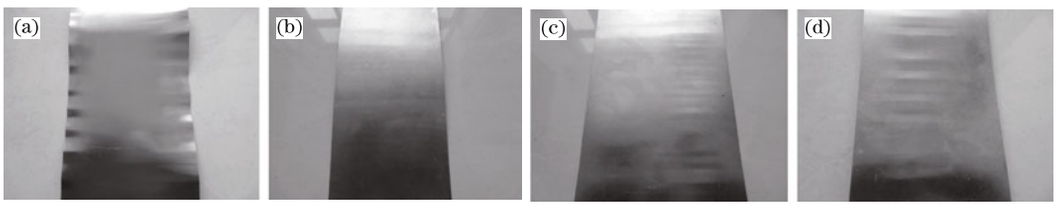

Fig. 8 Test results for different taper lengths of 30 mm (a), 50 mm (b), 60 mm (c) and 70 mm (d)

4 Conclusions

(1) Based on the boundary integral equation method, an analytical model for solving the finite length semi-infinite body is established. With the boundary integral equation method, a more accurate roll flattening analytical model is established. Compared with semi-infinite body model and Foppl formula, the result calculated by new model is more consistent with FEA. The new model is more accurate to predict the roll flattening, especially near the roll edges.

(2) Considering the cluster rolls character of 20-high mill and based on the new roll flattening model, a new 20-high mill plate shape control model is established. Based on the new model, the effects of the first intermediate roll taper angle and taper length are analyzed. The results show that changing first intermediate roll length (roll shifting) is more effective for plate shape control than changing the roll angle. In order to ensure a good plate shape, the taper has shift within the plate width range. The tension distribution calculated by analytical model is consistent with the test result.

References:

[1] H. L.Yu, X. H. Liu, C. Wang, H. D. Park, J. Iron Steel Res. Int. 15 (2008) No. 1, 30-33.

[2] R. J. Roark, Formulas for Stress and Strain, McGraw-Hill, New York, 1954.

[3] Y. Tozawa, M. Ueda, Journal of the Japan Society for Technology of Plasticity 11 (1970) No. 108, 29-37.

[4] H. L. Yu, X. H. Liu, G. T. Lee, Journal of Manufacturing Science and Engineering 130 (2008) No. 1, 0110161-0110167.

[5] J. H. Cho, S. M. Hwang, Journal of Manufacturing Science and Engineering –Transactions of the ASME 136 (2014) No. 1, 204-226.

[6] J. M. Shin, S. I. Han, J. S. Kim, J. Iron Steel Res. Int. 20 (2013) No. 12, 25-32.

[7] C. T. Wang, K. L. Fang, Steel Rolling 22 (2005) No. 4, 14-23.

[8] K. Hara, T. Yamada, K. Takagi, ISIJ Int. 31 (1991) 607-613.

[9] S. Timoshenko, Theory of Elasticity, McGraw-Hill, New York, 1951.

[10] B. Berger, O. Pawelski, P. Funke, Archive for the Iron and Steel Industry, Verlag Stahleisen, Berlin, 1976.

[11] S. X. Zhou, P. Funke, J. Zhong, Steel Res. 67 (1996) No. 5, 200-204.

[12] S. X. Zhou, P. Funke, J. Zhong, C. Plociennik, Steel Res. 67 (1996) No.11, 491-494.

[13] A. Hacquin, P. Montmitonnet, J. P. Guillerault, Eur. J. Mech. 17 (1998) No. 1, 79-106.

[14] J. Liang, K. M. Liew, Int. J. Numer. Meth. Eng. 52 (2001) No.11, 1189-1202.

[15] R. D. Mindlin, Physics 7 (1936) No. 5, 195-202.

[16] H. Xiao, Z. W. Yuan, T. Wang, J. Iron Steel Res. Int. 20 (2013) No. 10, 39-45.

[17] G. D. Wang, The Shape Control and Theory, Metallurgical Industry Press, Beijing, 1986.

[18] J. C. Lian, in: Proceeding of the First International Conference on Steel Rolling, Tokyo, 1980, pp. 713-724.

[19] C. J. Lu, Z. J. Liu, X. H. Liu, G. D. Wang, Research on Iron and Steel 46 (2000) No.3, 32-33.